A Hodoscope Study of Penetrating Cosmic-Ray Showers. II. Extensive Showers*

KURT SITTE
Physics Department, Syracuse University, Syracuse, New York
(Received February 1, 1950)

The interactions of penetrating particles in air showers have been studied with a hodoscope arrangement at an altitude of 3260 m. About 90 percent of all charged penetrating particles do not originate local showers of penetrating secondaries, and are absorbed only very slowly. This "non-interacting component," consisting at least predominantly of μ-mesons, has a rather flat range spectrum between 280 and 680 g/cm² Pb. Its zenith angle distribution is approximately proportional to $\cos^4\theta$. The remaining 10 percent constitute a "charged N component"; the total fast N component amounts to about one-fourth of the number of the charged penetrating particles. The collision mean free path of the fast N component was found to be (220±30) g/cm² if a minimum of 100-g/cm² penetration is demanded for the local showers. From the recorded increase of the number of shower particles with absorber thickness it is concluded that further multiplication after the first collision is quite common, and that the mean free path of the secondaries of local showers is not much larger than that of the primary N component.

I. ARRANGEMENT AND SHOWER SELECTION

DURING the last years, much progress has been made in our understanding of the complex phenomena connected with extensive showers. Thus, for instance, important questions like that of the place of the origin of the penetrating particles, or that of the existence of a new light fundamental particle, can be considered as definitely settled. In particular, the work of Cocconi, Tongiorgi, and Greisen[1] on penetrating particles in extensive air showers has clearly established that these particles are mainly μ-mesons which are produced not locally in the absorber surrounding the counter arrangement, but in air, possibly high above the apparatus. On the other hand, the occurrence of local production of groups of penetrating particles has likewise been proven, perhaps most conclusively in the cloud-chamber studies of Ise and Fretter,[2] and of Brown and McKay.[3] However, the relative frequency of such events in the showers, the mean free path of secondary production, and many other details have not yet been completely explored in these investigations. It was the purpose of the present study to obtain additional evidence mainly about the composition of the penetrating component of air showers.

The experimental arrangement was the hodoscope apparatus described in Part I, on local showers.[4] In addition to the "master pulse" trays A, B, and C of the "P-set" shown in Fig. 1 of Part I, extension trays D and E were used to select air showers. Tray D consisted of six counters of 2 in. diameter and 24 in. length, connected in three groups of two counters each, and was placed in about $2\frac{1}{2}$ m distance from the P-set. It was furthermore intended to discriminate between showers of large and small electron density with the help of a similar fifth tray E in about 10 m distance from the P-set, using additional neon lamps to indicate whether or not E was struck. No difference of statistical significance could, however, be established, so that in the following analysis all recorded air showers are included without discrimination as to their densities.

The master pulse used to sensitize the neon indicator lamp system was formed by coincidences $(1A+1B+3D)$, that is, at least one particle striking tray A, at least one particle striking tray B, and at least one particle striking each subgroup of the extension trays D or E were required. During the entire air shower experiment tray A was shielded with lead absorbers of not less than 170 g/cm² thickness, while tray D remained unshielded. Thus, the master pulse was formed if a particle capable of penetrating at least 280 g/cm², accompanied by an electron shower, struck the apparatus. It was not required that tray C was also struck; if the penetrating particle reached the bottom tray, an extra neon lamp was discharged to facilitate classification.

In view of the heavy shielding of the trays of the P-set on all sides the probability of cascade particles triggering the trays A and B is negligible. As far as side showers are concerned, the use of separate master counters and hodoscope counters offers an additional check on their contribution. Cascade particles which might penetrate the 6 to 7-in. Pb side absorber, and trigger the master pulse counters, would frequently fail to reach the hodoscope trays, and leave the picture taken with this master pulse blank, or at least one tray apparently not struck. During a total of about 1000 hr. of recording, only 11 such events, that is less than one-half percent of all recorded showers, were found, and they may well have been due to the inefficiency of the trays or of the neon lamp system. While these pictures were disregarded in the analysis, no correction for either high energy cascades or side showers was deemed necessary. The correction for chance coincidences between single penetrating particles (3.4 per sec. in the P-set) and air showers triggering D only (approximately 40 per hr.) was negligibly small because of the short resolving time of the circuits used (about 4 to 5 μsec.).

* The expense of constructing the equipment and of running the experiment were partly provided by an AEC contract.
[1] Cocconi, Tongiorgi, and Greisen, Phys. Rev. **75**, 1063 (1949).
[2] J. Ise and W. B. Fretter, Phys. Rev. **76**, 933 (1949).
[3] W. W. Brown and A. S. McKay, Phys. Rev. **76**, 1034 (1949).
[4] K. Sitte, Phys. Rev. **78**, 714 (1950).

TABLE I. Fraction $F(\theta)$ of non-interacting penetrating particles at zenith angle θ.

Mean zenith angle $\theta°$	0.9	4.0	7.1	10.2	13.3	16.2	19.1	22.0	24.7	27.2	29.7	32.0
Fraction F of showers	0.155	0.149	0.151	0.140	0.146	0.126	0.124	0.111	0.104	0.105	0.083	0.098

In general, the hodoscope pictures permitted a quite unambiguous distinction between the penetrating particles which traversed the apparatus without local production of penetrating secondaries, and those which originated groups of secondaries of considerable penetrating power. The first type of penetrating particles will be called the "non-interacting component," the latter the "interacting component." In order to be ranged among the interacting component, a penetrating particle had to be accompanied by secondaries which were observed at two consecutive levels, a and b, or b and c. Thus a penetrating power of the secondaries in excess of 100 g/cm^2, and in some cases in excess of 200 g/cm^2, was demanded, and hence the interacting component should include practically no electronic secondaries. This conclusion is born out in particular by the results of the experiment on local soft showers reported in the preceding paper. Local interactions apparent only at one level were ascribed to electronic secondaries of non-interacting penetrating particles. This interpretation was supported by the fact that they occur with about equal frequency at all three levels. It is possible that a small contribution of local penetrating showers initiated by N particles in the bottom absorber Σ_3 were included, but very few such particles should have escaped collisions in the upper layers Σ_1 and Σ_2.

II. RESULTS ON THE NON-INTERACTING COMPONENT

The pictures and records pertaining to the non-interacting component have been used to re-examine some of the properties of those particles. Evidence concerning the range distribution of the particles was the principal aim, but the zenith angle distribution had first to be studied before the ranges could be properly analyzed.

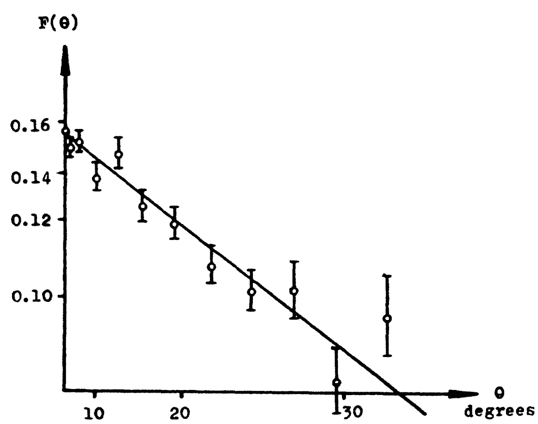

FIG. 1. Fraction $F(\theta)$ of showers of zenith angle θ, plotted against θ. The full line represents a distribution law $F(\theta)\propto\cos^{3.8}\theta$.

The frequency distribution of projected zenith angles θ was obtained from a total of 1592 single penetrating particles not accompanied by secondaries at any level. In evaluating it, correction has to be made for the geometrical bias of the arrangement which favors small zenith angles, and picks out a decreasingly small fraction of inclined particles. With 12 hodoscope counters at each level, one can define 12 zenith angle intervals and finds the distribution shown in Table I. (F is already corrected for the geometrical bias.) Plotting F against θ on a logarithmic scale, one obtains the curve depicted in Fig. 1. Unfortunately, the accuracy is rather low, but a distribution law of the form $N(\theta)\propto\cos^n\theta$ is in reasonable agreement with the experimental results for a value of $n=3.8\pm0.6$. The full curve of the graph represents this function. It is perhaps somewhat steeper than the $\cos^3$ law found by Brown and McKay;[4] the difference, if real, may be due to the fact that their statistics included all penetrating particles, and the present one only the non-interacting component.

The zenith angle distribution was needed to compute a correction that had to be applied in the evaluation of the range measurements, as the lowest tray did not cover the entire solid angle sustained by the master-pulse selecting trays A and B. If one calculates, with the angular distribution given above, the expected ratio of the flux through C to the flux through B in the absence of absorbers, one finds $N_C/N_B=0.74\pm0.03$. This was checked by a short run during which no absorber was placed between trays B and C, and coincidences $(1A+1C+3D)$ were recorded. The result was a ratio $N_C/N_B=0.81\pm0.1$. Therefore, the correction factor adopted was 0.76 ± 0.02.

Measurements were performed with three thicknesses of Σ_1: 170, 270, and 350 g/cm^2. During the first series of recordings, Σ_3 was 200 g/cm^2 throughout, and during the second 100 g/cm^2. The variation of Σ_3 has no influence on the master pulse; the over-all counting rates of the two runs are directly comparable. These are shown in Table II.

The last column gives the ratio of the recorded rates to that at top absorber thickness 170 g/cm^2 (total absorber thickness 280 g/cm^2), which was chosen as reference in all further analyses. The slow variation of R/R_{170} indicates the high penetrating power of the non-interacting component.

More evidence can then be added from the hodoscope records of tray c. These are summarized in Table III. The columns "N_{ab}" give the total number of non-interacting particles which penetrate to at least tray

TABLE II. Rate of extensive penetrating showers as function of the top absorber thickness α_1.

Absorber thickness (g/cm²)	Showers recorded	Recording time (hr.)	Shower rate R (hr.$^{-1}$)	R/R_{170}
170	686	292.5	2.35±0.09	1.0
270	697	327.0	2.13±0.08	0.91±0.07
350	769	388.5	1.98±0.07	0.84±0.07

TABLE III. Number of particles penetrating at least to tray b (N_{ab}) and to tray c (N_{abc}) for different top absorber thicknesses Σ_1.

Absorber thickness (g/cm²)		$\Sigma_1=170$ g/cm² N_{ab}	N_{abc}	$\Sigma_1=270$ g/cm² N_{ab}	N_{abc}	$\Sigma_1=350$ g/cm² N_{ab}	N_{abc}
Particles	$\Sigma_3=100$	438	309	452	310	479	316
Recorded	$\Sigma_3=200$	462	295	481	283	530	310

b, and those headed "N_{abc}" the number of particles recorded at c.

In order to use these figures for a determination of the range spectrum of the non-interacting component, the readings at the c tray have to be corrected for losses due to the smaller solid angle sustained by this tray. This was done with the correction factor given.

From the values shown in Table III, a differential range spectrum can be computed over the range intervals (in g/cm²) 280–400 and 280–500, 380–500 and 380–600, 460–580 and 460–680. Using the results of the shorter first interval of each group to subdivide the second, and combining the results of approximately equal range intervals, one can, with a slight adjustment of the interval limits, rearrange the data in four groups: 280–380, 380–480, 480–580, and 580–680 g/cm². The values of Table II furnish additional material, so that all intervals except the last are covered by at least two observations. This procedure, though of questionable correctness, appears to be adequate within the accuracy attainable in the present experiment. The results are presented in the graph of Fig. 2, in which the fraction of non-interacting particles absorbed in range intervals of 100 g/cm² is plotted against the range of the particle. As a second scale the momentum of the particle is shown, taken from the range-momentum curves of E. P. Gross under the assumption that the non-interacting penetrating particles are μ-mesons.

Figure 2 shows that the differential momentum spectrum of the penetrating shower particles in the region between about 450 to 900 Mev/c is rather flat. A very appreciable fraction, probably about 40 percent, of all particles of momentum exceeding the minimum penetration of 280 g/cm²≈450 Mev/c has a momentum of less than 1 Bev/c.

Finally, the frequency distribution of groups of non-interacting penetrating particles was registered. There was no significant variation with the absorber thickness Σ_1, the average over all three runs showing single particles in (75±2) percent of all showers; pairs of particles in (16.6±0.9) percent of all showers; triples in (6.3±0.5) percent of all showers; and larger groups in (2.2±0.3) percent of all showers; with an over-all average of (1.37±0.03) penetrating particles per shower.

III. RESULTS ON THE INTERACTING COMPONENT

A particle was called interacting if it was accompanied by at least one secondary at one hodoscope level a, b, or c, and by at least two secondaries at a neighboring level. Electron cascades would only be recorded as interacting if they contain still at least two charged particles under Σ_1 and Σ_2: an entirely negligible contribution. Triple knock-ons of non-interacting particles would be included, but amount to much less than 0.1 percent of the meson component, and this is less than the accuracy attainable in the present analysis. Therefore, one can be satisfied that practically all the particles classified as "interacting" belong to the N component, and that the "interaction" selected consisted in the ejection of at least one secondary capable of penetrating more than 100 g/cm² Pb (or, in part of the experiment, more than 200 g/cm² for local events originating in Σ_2), together with others of lower penetration.

The summary of the observations on interacting particles is given in Table IV. Local showers are subdivided into "Σ_1-showers"; that is, those originating in the top absorber Σ_1, and "Σ_2-showers" originating in the middle absorber Σ_2. One realizes that the arrangement will record Σ_1-showers initiated by both charged and neutral particles, but discriminates against neutral primaries of Σ_2-showers. Such events will be recorded only if a charged secondary, emitted backward, strikes one of the A counters. In general it is possible to distinguish between the two different events; in the present analysis of 33 Σ_2-showers 23 were clearly recognized as produced by charged N particles, and six as due to neutral particles, with only four classified as uncertain. As these "uncertain" showers cannot be disregarded in the following statistical analysis, they were assigned to the two groups in, as near as possible,

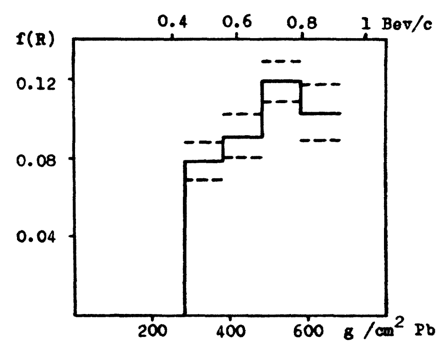

FIG. 2. Fraction f(R) of non-interacting penetrating particles of range between R and (R+100) g/cm² Pb. The dotted lines indicate the probable errors. [*Note added in proof:* Through an unfortunate mistake the dotted lines in Fig. 2 do not show the correct relative errors. The true errors are larger; the values of $f(R)$ in the four intervals are: 7.8±4.8, 9.1±2.4, 11.9±2.3, 10.3±2.0.]

TABLE IV. Rate of local penetrating showers produced by "interacting" penetrating air-shower particles in the top absorber (Σ_1-showers) and in the middle absorber (Σ_2-showers).

Σ_1 (g/cm²)	Time (hr.)	Σ_1-showers Number	Rate/hr.	Σ_2-showers Number	Rate/hr.
170	280.5	90	0.321 ± 0.033	12(15)	0.043 ± 0.012
270	324.0	139	0.428 ± 0.036	8(11)	0.025 ± 0.018
350	373.0	172	0.462 ± 0.036	6(7)	0.016 ± 0.006

the frequency ratio of the identified showers. This brings the total of neutral primaries to seven against 26 charged particles, and increases the experimental uncertainties somewhat beyond the statistical errors. In column 5 of Table IV, the first figures refer to the number of Σ_2-showers initiated by charged N particles, and those in brackets are the total of all observed Σ_2-showers

It should be noted that the Σ_2-showers of the air shower experiment are related to the events (LPS+E) of the preceding report[4] on local showers. These events are included in the Σ_2-showers; they required at least three penetrating shower particles, while in the selection of Σ_2-showers only two such particles were demanded, plus one of less penetration. Consequently, the rates $R_{\Sigma 2}$ are considerably higher than those of the events (LPS+E). But even with the less stringent selection the flux of N particles in air showers is obviously much smaller than that of the shower-producing particles not accompanied by an extensive shower. If we exclude primary electrons as the source of air showers, it would then follow that only a small fraction of those primaries which initiate nucleonic showers will simultaneously give origin to electronic showers of the density recorded in this arrangement. The process in which, directly or indirectly, electrons are released in nuclear collisions (including radiation) must either be infrequent for all energies, or be more or less confined to very high primary energies.

The rate $R_{\Sigma 1}$ of Σ_1-showers can be used immediately for a determination of the flux R_N of N particles in the extensive showers, and of the collision mean free path λ of those particles. It is assumed that the efficiency of the apparatus for recording an interaction with at least one penetrating secondary is practically unity; this assumption is supported strongly by the evidence of the hodoscope records, which show in general too high a multiplicity of the events to make a miss likely. If one then tries to fit the experimental rates to the expression one obtains for the shower rate under the assumption of a uniform collision mean free path:

$$R_{\Sigma 1}=R_N[1-\exp(-\Sigma_1/\lambda)]$$

with the least deviation, one finds $R_N=(0.59\pm0.03)$ hr.$^{-1}$, and $\lambda=(220\pm30)$ g/cm². The results are reproduced in Fig. 3: the observed shower rates by circles and the rates calculated with the values quoted above by the full curve.

In a similar way, one can derive, though rather inaccurately, a value for the flux R_p of charged N particles from the rates of Σ_2-showers. This quantity should be obtained from $R_{\Sigma 2}$ by using the expression:

$$R_{\Sigma_2}=R_p\exp(-\Sigma_1/\lambda)\cdot[1-\exp(-\Sigma_2/\lambda)].$$

Taking the three values of Table IV, one has an average of $R_p=(0.234\pm0.05)$ hr.$^{-1}$, or very nearly one-half of the value for the entire N component.

The main interest is then in a comparison of these rates with the rate of μ-mesons in extensive showers, measured in the flux of non-interacting particles. Several corrections have to be applied to the data given in the preceding section, in order to avoid a number of possible systematical errors. First of all, the number of "non-interacting" showers is not equal to the number of non-interacting particles, and the same is true for the "interacting" showers. In the former case, we have found about 1.4 penetrating particles per shower. In the latter, a precise analysis of the density distribution of interacting particles is not possible. Whenever several N particles hit the absorber, the resulting shower is so dense that it defies attempts to trace individual particles. An exception is the run with the smallest top absorber thickness, $\Sigma_1=170$ g/cm², where one has a reasonable certainty of distinguishing pairs or groups of incident particles from single primaries. Of the 90 analyzed Σ_1-showers, 62 were clearly recognized as due to events in which only one penetrating particle struck the absorber, while in 10 cases the shower primary was accompanied by another penetrating particle, and 18 showers were too complex for an identification. Thus, it appears that the density distribution of the N particles does not differ very markedly from that of the meson component, and the rates of "interacting" and "non-interacting" showers can be taken as measure of the relative frequency of the two components.†

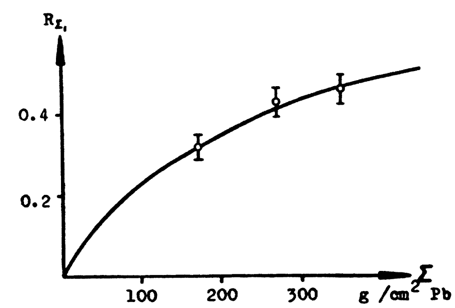

FIG. 3. Rate $R_{\Sigma 1}$ of Σ_1-showers against top absorber thickness. The curve is calculated from $R_{\Sigma 1}=R_0(1-e^{-\Sigma/\lambda})$, with $R_0=0.59$ hr.$^{-1}$ and $\lambda=220$ g/cm².

† The observation has been made that groups of penetrating particles appear to initiate local showers with a larger probability per particle than do single particles, and the explanation offered that such groups, incident on a comparatively small area, would most likely come from the neighborhood of the apparatus, so that the π-mesons in the group have not yet decayed, and the group consists more or less entirely of N particles. The probability of detecting such groups, however, depends strongly on the area of the collecting trays. For the dimensions used in this experiment one can show that fewer than one percent of the recorded events

A second correction of the flux of non-interacting particles comes from the fact that some of the N particles will escape collisions in both Σ_1 and Σ_2, and hence be classified as non-interacting. Their contribution can be calculated, with the rates and the collision mean free path given above, and subtracted from the the observed flux. It may be added that the correction is much too small to make the systematical error, introduced in the range distribution of Fig. 2 by the inclusion of these particles, comparable with the statistical errors.

Third, some mesons will arrive in groups containing N particles, and are excluded if the meson flux is computed from the rate of "non-interacting" showers only. Again this correction can be calculated if one assumes the same density distribution of both components; it turns out to be small, but not negligible.

The standard of comparison used in the following discussion is the μ-meson flux under the minimum penetration condition imposed in this experiment, that is under a total of 280 g/cm^2 or about 10 in. Pb. With all three corrections applied, this flux is 2.23 ± 0.09 hr.$^{-1}$, and from this one obtains for the ratio of the total N component to the μ-meson component:

$$N_N/N_\mu = 0.26\pm0.03,$$

and for the ratio of the charged N component to the μ-meson component:

$$N_P/N_\mu = 0.105\pm0.022.$$

It is interesting to note that this ratio is more than 10 times larger than that of the primary flux at 700 g/cm^2, computed from the incident flux with the help of Tinlot's[5] absorption thickness, to the μ-meson flux at the same altitude. Even if a somewhat slower absorption of the N component recorded in this experiment were assumed, as the interactions selected were not very energetic (see Rossi[6]), the difference would remain significant. In other words: If one defines an "average multiplicity of meson production" as the ratio of the total μ-meson flux, that is, the sea-level flux corrected for decay while traversing the atmosphere, to the flux of cosmic-ray primaries, one obtains a value of about 0.1. If one defines, similarly, an average multiplicity of meson production in showers as the ratio of μ-meson flux to the flux of the N component, both re-projected to a producing layer near the top of the atmosphere, he finds a much lower value. This indicates that most collisions of nucleons of moderate energies will result in the ejection of a small number of nucleonic secondaries of moderate penetration, without the production of meson secondaries. Alternatively, one might conclude that the bulk of the showers is produced not near the top of the atmosphere, but at much lower altitudes.

Mention has already been made repeatedly of the frequent complexity of local showers in dense absorbers. This undoubtedly demonstrates the occurrence of "cascades" of nuclear collisions, already well-known from cloud-chamber pictures. While a complete analysis of such entangled events is not possible from a hodoscope picture, some conclusions can be drawn from a statistical analysis based on the records of the numbers of counters struck under a certain absorber thickness. This method faces a serious objection: The number of counters struck is, in a dense shower, certainly not equal to the number of particles present, and this second quantity is the one which should be discussed. Moreover, a method of deducing the latter number from the first cannot be worked out unless the spacial distribution of secondaries in the shower is known. However, the correction will be small if the particle density is not too high, while for very large densities, which in general will occur only if several local events contribute, the resulting distribution cannot be far from random. Hence one can expect that the observed numbers, corrected under the assumption of random distribution of the shower particles, will for all densities deviate very little from the true numbers. Writing $P(m, n, N)$ for the probability that a shower of m particles discharges n out of a tray of N counters, one has then

$$P(m, n, N) = \binom{N}{n}\cdot p^n\cdot(1-p)^{N-n},$$

where p is the probability that one counter is discharged. From this, the average number $\langle n\rangle$ of counters struck can be calculated as a function of m, and by comparison with the experimental values the most probable number $\langle m\rangle$ of particles present can be evaluated. The results are given in Table V. In computing the number of

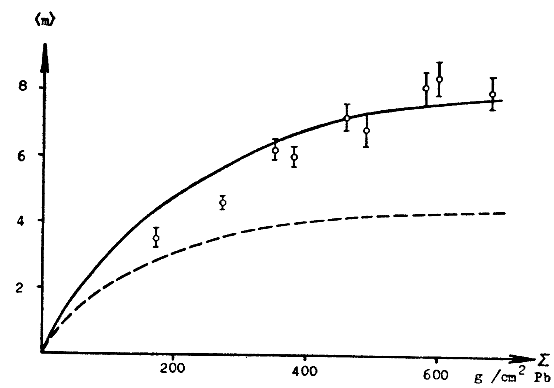

FIG. 4. Average number $\langle m\rangle$ of particles in all Σ-showers against absorber thickness. The full curve represents exponential increase with $\lambda = 220$ g/cm^2, normalized to optimum agreement at large thicknesses. The dotted curve represents the same exponential law, with an asymptotic value $m_0 = 4.7$.

is due to groups of N particles. This is considerably less than the number of groups of three or more particles of unrelated origin which one would expect in dense showers, or the number of groups due to density fluctuations. It might, though, be that at least some of the disputed "narrow showers" [see J. Wei and C. G. Montgomery, Phys. Rev. **76**, 1488 (1949)] with their peculiar features are indeed such groups of N particles.

[5] J. Tinlot, Phys. Rev. **73**, 1476 (1948); **74**, 1197 (1949).

[6] B. Rossi, M.I.T. Technical Report No. 26 (April 4, 1949).

TABLE V. Average number $\langle m \rangle$ of particles observed in local showers produced by the "interacting" component, as function of the absorber thickness. $\langle m \rangle$ is calculated from the number $\langle n \rangle$ of counters struck under the assumption of random distribution.

Absorber thickness (g/cm^2)	170	270	350	380	460	490	580	600	680
Number $\langle m \rangle$ of shower particles	3.5 ± 0.3	4.6 ± 0.2	6.2 ± 0.3	6.0 ± 0.3	7.2 ± 0.4	6.8 ± 0.5	8.1 ± 0.5	8.4 ± 0.5	8.0 ± 0.5

particles hitting the lowest tray, a further correction for the reduced solid angle has been made, using the same efficiency factor as in the range determination of the preceding section.

The results are again represented in the graph of Fig. 4 in which the average number of shower particles ejected in collisions of the interacting component is plotted against the absorber thickness traversed. Evidently, if after the first collision no further "cascade" multiplication occurs, the average number of particles observed under an absorber of thickness Σ is

$$\langle m \rangle = m_0(1-e^{-\Sigma/\lambda})$$

(m_0 = number of particles emitted per collision). The same law holds even if further multiplication does occur, but with a mean free path much larger than that for the first collision. Other, more complex, formulas can be derived if secondary and higher interactions follow the first with a comparable mean free path, and equal or different multiplicities, but it would require a much higher accuracy than that attained in the present experiment for precise quantitative conclusions to be deduced in this way. Only one general feature of such "cascades" should be kept in mind: If absorption is neglected, the number of particles after two steps should approach a saturation value $\langle m \rangle = m_0 \cdot n_0$, if m_0 and n_0 are the multiplicities of the first and second collision.

The full curve in Fig. 4 shows an attempt at representing the measured particle densities by a single exponential increase with the previously determined value of $\lambda = 220$ g/cm^2, normalized so as to give optimum agreement at larger thicknesses. The dotted curve is calculated with an initial multiplicity $m_0=4.7$, the average value observed for unaccompanied local showers of similar penetration. In both cases the disagreement is obvious. The observed numbers increase to values which are extremely unlikely for events of rather low energy, and not at all according to a single exponential law. The conclusion appears inevitable that further multiplication does take place, and with a mean free path of the same order as that of the first step; certainly much smaller than 500 to 600 g/cm^2, as for still thicker absorbers little, if any, additional shower production occurs. Furthermore, it appears likely that the multiplicity in the later steps is smaller than in the first: $m \cdot n \gtrsim 8$, while probably $m \sim 4$. It may, of course, be that not all of the secondaries are capable of further multiplication; a feature which could also explain the discrepancy between the larger values, about 750 g/cm^2, of the mean free path of secondaries obtained from cloud-chamber data (e.g., Fretter[7]) and the present estimates. One cannot safely draw more than the qualitative conclusion that whatever "cascade" multiplication of nuclear collisions occurs will be characterized by a collision mean free path which does not vary appreciably throughout the cascade development.

IV. SUMMARY

The hodoscope technique has been found to be a convenient method for distinguishing between "interacting" and "non-interacting" penetrating particles in air showers. The latter component, at least in the bulk μ-mesons, has a rather flat range distribution in the energy interval between 350 and 800 Mev, with about 40 percent of all particles having energies below 1 Bev. The zenith angle distribution of the non-interacting component follows approximately a law of the form $\cos^n\theta$ with $n=3.8\pm0.6$. For those of the "interacting" particles which originate showers of at least three secondaries at two consecutive levels (showers which strike at least five hodoscope counters) a collision mean free path of (220 ± 30) g/cm^2 is found. Further nuclear collisions occur with apparently not much changed mean free path, but possibly fewer secondaries, if all or most of the particles ejected in the first collision contribute to the developing "cascade" of nuclear events. From the observed flux of non-interacting particles, $R_\mu = (2.23\pm0.09)$ hr.$^{-1}$, the flux of all interacting particles, $R_N = (0.59\pm0.03)$ hr.$^{-1}$ and the flux of charged interacting particles, $R_p = (0.23\pm0.05)$ hr.$^{-1}$, one computes that in air showers, at 3260-m altitude, there are about four μ-mesons present for each N particle, or about 10 μ-mesons per charged N particle. This is considerably less than the ratio of single μ-mesons to shower-producing nucleons at the same altitude, suggesting that N particles of moderate energies would in general still be capable of ejecting "knock-on protons" in nuclear collisions, while no longer producing mesons.

In conclusion the author wishes to thank the Inter-University High Altitude Laboratories, and particularly Drs. Cohn and Iona of the University of Denver, for the permission to use the facilities at Echo Lake Laboratories.

[7] W. B. Fretter, Phys. Rev. 76, 511 (1949).